

Catalytic Efficacy of Copper(II)– and Cobalt(III)–Schiff Base Complexes in Alkene Epoxidation

Monami Maiti,[1] Dipali Sadhukhan,[1] Santarupa Thakurta,[1] Ennio Zangrando,[2] Guillaume Pilet,[3] Sandra Signorella,[4] Sebastián Bellú,[4] and Samiran Mitra*[1]

[1]Department of Chemistry, Jadavpur University, Raja S. C. Mullick Road, Kolkata-700032, India

[2]Department of Chemical and Pharmaceutical Sciences, Via Licio Giorgieri, 1 34127 Trieste, Italy

[3]Groupe de Crystallographie et Ingénierie Moléculaire, Laboratoire des Multimatériaux et Interfaces, UMR 5615 CNRS-Université Claude Bernard Lyon 1, Bât. Chevreul, 43 bd du 11 Novembre, 1918, 69622 Villeurbanne, Cedex, France

[4]Instituto de Química Rosario (IQUIR)-CONICET, Facultad de Ciencias Bioquímicas y Farmacéuticas, Universidad Nacional de Rosario, Suipacha 531, S2002LRK Rosario, Argentina

Received December 3, 2013; E-mail: smitra_2002@yahoo.com

A potentially hexadentate N_2O_4 donor Schiff base ligand *N*,*N*′-bis(5-bromo-3-methoxysalicylideneimino)-1,3-diaminopropane (H_2L^1) has been used to synthesize two mononuclear coordination complexes $[Cu(L^1)]\cdot H_2O$ (**1**) and $[Co(L^1)(HL^2)]ClO_4\cdot CH_3CN$ (**2**). The cobalt complex is a unique mixed-ligand species comprising both the di- and mono-condensed ligands; the latter (HL^2) resulted from in situ hydrolytic cleavage of H_2L^1. Ligand L^1 assumes a planar arrangement in **1** and a folded β-*cis* configuration in **2**, induced in this case by the chelating HL^2 ligand. The complexes are characterized by elemental analyses, FT-IR, and UV–vis spectral methods, and their structures are established by single-crystal X-ray diffraction study. Both the complexes are proven to be efficient catalysts for the epoxidation of alkenes by H_2O_2 or PhIO. The efficiency of alkene epoxidation is however somewhat superior with PhIO, and in each case, **2** appears to be a slightly better catalyst than **1**.

A large number and a variety of Schiff base complexes have been studied in connection with a number of possible applications which range from their ability to reversibly bind oxygen,[1] to catalytic activity in hydrogenation of olefins[2] as well as transfer of an amino group,[3] and photochromic properties.[4] Tetradentate di-condensed ligands such as salen/salpn-type Schiff bases are quite capable of forming complexes with certain metal ions, which can exhibit unusual coordination, high thermodynamic stability and kinetic inertness.[5–8] On the other hand, the most challenging step for the construction of mono-condensed Schiff base ligands is to selectively condense only one primary amine group of the diamine to form an imine bond.[9–11] The existence of a di- or mono-condensed Schiff base during a particular reaction can be modulated by the geometric preferences of the metal ion present in the medium. Consequently, the coordination geometry of the resulting complex depends upon the electronic configuration and size of metal ion, the type of other auxiliary ligands present in the coordination sphere, the inherent rigidity due to the presence of aromatic rings, etc.[12] The resulting topologies are also based on strong metal–ligand covalent bonds[13,14] and multiple weak noncovalent forces like hydrogen bonding[15,16] and π–π interactions.[17–19]

Epoxidation of alkenes represents a fundamental reaction in industrial organic synthesis[20] because epoxides are key intermediates for the manufacture of a wide variety of valuable products, both bulk[21] and fine chemicals.[22] Despite the enormous research efforts dedicated to the development of efficient catalysts for alkene oxidation, some problems remain, in particular, those concerning the nature of the oxidant and the product selectivity. Thus, the search for efficient, selective, and environmentally benign catalysts for these oxidation reactions is currently an important synthetic goal.[23] Although historically [Mn(salen)] complexes[24–26] were considered as important candidates for epoxidation of alkenes, recently some mono- and dinuclear Ni(II) Schiff base–macrocyclic complexes have been used for this purpose.[27] Copper(II) Schiff-base complexes, upon immobilization into microporous or mesoporous aluminosilicates, have been also found capable to catalyze olefin epoxidations.[28–30] However, the activity of Schiff-base complexes of Cu(II) or Co(III) toward catalytic oxidation in homogeneous medium is not well documented in the literature.[31–37] The catalytic efficiency of Cu(II)/Co(III) complexes depends on the nature of terminal oxidants as well as on the specific ligand environment.

In order to explore the use of metal templates[38] in controlling the coordination pattern of Schiff base ligands, we have synthesized a symmetric, di-condensed ligand H_2L^1 (Figure 1) and investigated the influence of copper and cobalt ions on the stability of this ligand. We report herein the synthesis and structural characterization of two mononuclear complexes, $[Cu^{II}(L^1)]\cdot H_2O$ (**1**) and $[Co^{III}(L^1)(HL^2)]ClO_4\cdot CH_3CN$ (**2**) and the catalytic ability of these complexes toward the epoxidation of various alkenes. Although complex **1** was very recently structurally characterized by Cristóvão et al.,[39] in the present work we account for this square-planar Cu(II) complex to place

Published on the web April 4, 2014; doi:10.1246/bcsj.20130334

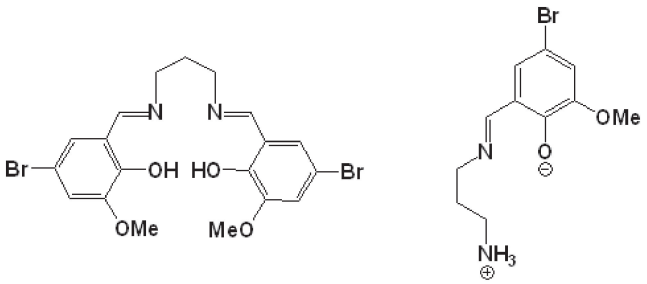

H_2L^1 HL^2

Figure 1. Perspective view of the di- and mono-condensed Schiff base ligands.

emphasis on the catalytic efficiency and structure–function correlation in alkene epoxidation with respect to the octahedral Co(III) complex, where the salen ligand adopts a different configuration.

Experimental

Syntheses. All chemicals and solvents employed for the syntheses were of analytical grade and used as received without further purification. 5-Bromo-*o*-vanillin (i.e., 5-bromo-2-hydroxy-3-methoxybenzaldehyde) and 1,3-propylenediamine (i.e., 1,3-diaminopropane) were purchased from Aldrich Chemical Co. Copper(II) acetate monohydrate was purchased from Loba. Cobalt(II) perchlorate hexahydrate was prepared by the treatment of cobalt carbonate (E. Merck, India) with 80% perchloric acid (E. Merck, India) followed by slow evaporation. It was then filtered through a fine glass-frit and preserved in $CaCl_2$ desiccator. *Caution!* Perchorate salts are potentially explosive and should be handled with much care and in small amount, though no problem was accounted.

Synthesis of $[Cu(L^1)]\cdot H_2O$ (1). The ligand H_2L^1 was prepared following a method reported in literature.[40] $Cu(CH_3COO)_2\cdot H_2O$ (0.199 g, 1 mmol) was dissolved in 20 mL of MeOH followed by the addition of 10 mL of yellow methanolic solution of H_2L^1 (1 mmol, 0.502 g). The mixture was stirred for 30 min at 40 °C. The dark green solution was kept in a refrigerator at 16 °C. After one day brown needle-shaped single crystals suitable for X-ray diffraction were obtained. Yield: 0.493 g (85%). Elemental analysis. Found: C, 39.38; H, 3.40; N, 4.79%. Calcd for $C_{19}H_{20}Br_2Cu_1N_2O_5$ (579.73): C, 39.36; H, 3.48; N, 4.83%. FT-IR bands. $\nu_{(C=N)}$ 1610, $\nu_{(C-O_{Phenolic})}$ 1226, $\nu_{(Cu-N)}$ 438 cm^{-1}. ESI-MS. m/z $[Cu(L^1)] = 562$.

Synthesis of $[Co(L^1)(HL^2)]ClO_4\cdot CH_3CN$ (2). $Co(ClO_4)_2\cdot 6H_2O$ (1 mmol, 0.366 g) was dissolved in 10 mL of CH_3CN. 10 mL of methanolic solution of the Schiff base H_2L^1 (2 mmol, 1.004 g) was added to this solution. The mixture was stirred for 30 min at a temperature of 40 °C. Then the resulting dark brown solution was kept at room temperature. Orange square-shaped single crystals suitable for X-ray diffraction were obtained within two days. Here, the ligand HL^2 (Figure 1) has not been prepared separately; rather it is formed in situ by the hydrolytic cleavage of H_2L^1. Yield: 0.709 g (72%). Elemental analysis. Found: C, 38.90; H, 3.62; N, 7.09%. Calcd for $C_{32}H_{36}Br_3Cl_1Co_1N_5O_{10}$ (984.77): C, 39.03; H, 3.68; N, 7.11%. FT-IR bands. $\nu_{(C=N)}$ 1591, $\nu_{(C-O_{Phenolic})}$ 1234, $\nu_{(O-H)}$ 3432, $\nu_{(N-H)}$ 3232–3148, $\nu_{(ClO^{4-})}$ 1081, $\nu_{(Co-N)}$ 459 cm^{-1}. ESI-MS. m/z $[Co(L^1)(HL^2)]^+ = 844$.

Physical Measurements. The FT-IR spectra of the compounds were recorded on a Perkin-Elmer RX I FT-IR spectrometer with KBr pellets in the range 4000–400 cm^{-1}. The electronic spectra were recorded at 300 K on a Perkin-Elmer Lambda 40 (UV–vis) spectrometer using HPLC grade acetonitrile as solvent in the range 800–200 nm. Elemental analyses were carried out on a Perkin-Elmer 2400 II Elemental Analyzer. Electrochemical studies were performed on a VersaStat-PotentioStat II cyclic voltammeter using HPLC grade acetonitrile as solvent where tetrabutylammonium perchlorate was used as supporting electrolyte at different scan rates. Platinum and saturated calomel (SCE) were the working and the reference electrodes in the process, respectively. Mass spectra of both the complexes were analyzed in a Qtof Micro YA263 mass spectrometer. HPLC experiments were performed with a Varian ProStar chromatograph equipped with DAD 335 detector using a Varian Microsorb-MV 100–5 C18 column (250 × 4.6 × 1/4"), with a Zeltec thermostatted heater. Samples were eluted with a 70:30 acetonitrile/methanol mixture at a flow rate of 0.4 mL min^{-1} at 40 °C. Under these experimental conditions, retention times t_R were as it follows: styrene (t_R = 7.88 min), styrene epoxide (t_R = 7.17 min), *cis*-stilbene (t_R = 8.51 min), cyclohexene (t_R = 9.47 min), cyclohexene oxide (t_R = 7.13 min), *trans*-4-octene (t_R = 11.39 min). Calibration curves of authentic alkene and product samples were used to quantify the alkene conversion and product selectivity. At least two independent experiments were performed for each set of reaction conditions. Blank experiments with the oxidant using the same experimental conditions except catalyst were performed. Alkene conversion in absence of the complex was 0–5%.

Crystal Data Collection and Refinement. Intensity data of **1** were collected at 293 K using Mo Kα radiation (λ = 0.71069 Å) with an Oxford Diffraction Gemini diffractometer, while the data collection of **2** was carried out on a rotating anode diffractometer equipped with Kappa-CCD plate and Cu Kα radiation (λ = 1.54178 Å). CrysAlis RED[41] and Denzo/Scalepack[42] programs were used for data reduction of **1** and **2**, respectively. The structures were solved by direct methods using the program SIR97[43] and SHELXS-97[44] and refined by full-matrix least-squares methods with programs CRYSTALS[45] and SHELXL-97[44] for **1** and **2**, respectively. The Δ Fourier map of **2** revealed the presence of a lattice CH_3CN molecule. Being this molecule rather disordered, it was refined with restrained thermal parameters. All the H atoms were generated geometrically and included in the final cycles of refinement with the riding model approximation. Selected crystallographic data, experimental conditions, and relevant features of the structural refinements for the structures of **1** and **2** are summarized in Table S1 and Table 1, respectively.

Crystallographic data have been deposited with Cambridge Crystallographic Data Centre: Deposition number CCDC-890124 and 890125 for **1** and **2**. Copies of the data can be obtained free of charge via http://www.ccdc.cam.ac.uk/conts/retrieving.html (or from the Cambridge Crystallographic Data Centre, 12, Union Road, Cambridge, CB2 1EZ, U.K.; Fax: +44 1223 336033; e-mail: deposit@ccdc.cam.ac.uk).

Catalysis Experiments. In one set of experiments, 150 μL of 10 M H_2O_2 (1.5 mmol) was added to a stirred solution of 2 μmol of catalyst (1.0 mg of **1** or 2.0 mg of **2**) and 0.8 mmol of alkene (82 μL of cyclohexene, 126 μL of *trans*-4-octene, 140 μL of *cis*-stilbene, or 92 μL of styrene) in 4 mL of freshly distilled CH_3CN, at a controlled temperature of 0 °C. In another set of experiments, to a stirred solution of 2 μmol of catalyst and 0.5 mmol of alkene (52 μL of cyclohexene, 79 μL of *trans*-4-octene, 87 μL of *cis*-stilbene, or 57 μL of styrene) in 4 mL of freshly distilled CH_3CN, 220 mg of PhIO (1.0 mmol) was added, at a controlled temperature of 20 °C. In each case, the reaction mixture was stirred at constant temperature, and the reaction time for maximal conversion was determined by withdrawing periodically aliquots of 10 μL from the reaction mixture, which were subjected to HPLC analysis. For oxidation with PhIO, a reaction time of 2 h was taken to calculate turnovers (converted mol/mol catalyst). At the end of the reaction, one aliquot was extracted from the aqueous layer. Aliquots were diluted with CH_3CN and filtered through a 0.2 μm membrane prior to injection into the chromatograph. In every case, the epoxide was the only reaction product.

Results and Discussion

Infrared and Electronic Spectra. Complexes **1** and **2** show similar IR features, with a strong band observed between 1591–1610 cm^{-1} attributable to imine ($\nu_{C=N}$) stretching band, which is 44–25 cm^{-1} lower than the corresponding band in the free ligand. A shift in the phenolic C–O stretching to a lower frequency with respect to the free ligand indicates the deprotonation and coordination of the phenolic oxygen donors to the metal center. Ligand coordination to the metal center can further be substantiated by prominent ν_{M-N} bands in between 438–459 cm^{-1} in the respective spectra of complexes **1** and **2**. The presence of a broad band in the IR spectra of **1** at about 3400 cm^{-1} is associated with lattice water molecule. For complex **2**, sharp bands are observed near 3232 and 3148 cm^{-1}, which can be assigned to ν_{N-H} stretching vibrations of NH_2 group. In addition, the IR spectrum of **2** gives a clear evidence of the presence of the protonated amine since the absorption band centered at 3148 cm^{-1} is characteristic of the ν_{N-H} vibration of the $-NH_3^+$ group. The characteristic absorption band for perchlorate anion appeared at 1081 cm^{-1} in the spectrum of **2**. The stretching vibrations of the free ligand and those of complexes **1** and **2** are listed in Table 2.

Table 1. Crystal Structure Parameters of $[Co(L^1)(HL^2)]$-$ClO_4 \cdot CH_3CN$ (**2**)

Empirical formula	$C_{32}H_{36}Br_3Cl_1N_5O_{10}Co$
Formula weight	984.77
Crystal system	Monoclinic
Space group	*I*2/*a*
a/Å	21.752(5)
b/Å	15.279(5)
c/Å	23.168(4)
β/degree	102.277(16)
V/Å^3	7524(3)
Z	8
D_{calcd}/Mg m^{-3}	1.739
μ/mm^{-1}	8.490
F(000)	3936
θ range/deg	3.5–63.0
Total data	41383
Unique data	5951
Obs data [$I > 2\sigma(I)$]	2858
*R*1[$I > 2\sigma(I)$]	0.0584
*wR*2[$I > 2\sigma(I)$]	0.1516
GoF	1.022
R_{int}	0.0840
Residuals/e.Å^{-3}	1.05, −0.81

The electronic spectral data for complexes **1** and **2** in HPLC grade acetonitrile solvent are in good agreement with their geometry. The strong absorption bands in the region 370–390 nm are clearly charge transfer in origin attributed to the transition from the coordinated unsaturated ligand to the metal ion (LMCT). Again, the intense high energy bands at about 262 and 325 nm for **1** and at 292 and 345 nm for **2** may be assigned to the intraligand $\pi \rightarrow \pi^*$ and $n \rightarrow \pi^*$ transitions, respectively. The broad low-intensity absorption band centered at 595 nm in the spectrum of complex **1** is a typical d–d band, structurally well characterized for square-planar copper(II) complexes.[46] For **2**, the band at 570 nm results from an $^1A_{1g} \rightarrow {}^1T_{1g}$ transition; typical d–d band of a Co^{III} in a distorted octahedral environment. The lower energy band $^1A_{1g} \rightarrow {}^1T_{2g}$ is probably obscured by the charge transfer band in the region 360–410 nm.

Cyclic Voltammetric Studies of 1 and 2. The electrochemical behavior of **1** and **2** were studied in HPLC grade acetonitrile medium with tetrabutylammonium perchlorate as supporting electrolyte at a scan rate of 100 mV s^{-1}. The cyclic voltammogram of **1** (Figure 2) shows two reduction peaks E_{pc1} (−0.09 V) and E_{pc2} (−1.06 V) during the cathodic scan. E_{pc1} corresponds to $Cu^{II} \rightarrow Cu^{I}$ reduction of the CuL^1 species. Some Cu^{I} ions generated in this process are absorbed on the electrode surface and are further reduced to metallic copper at E_{pc2}.[47] In the anodic side, the complex shows a strong stripping oxidation peak at $E_{pa1} = +0.101$ V which corresponds to the composite processes of $Cu^0 \rightarrow Cu^{II}$ and $Cu^{I} \rightarrow Cu^{II}$ oxidation. An additional oxidation peak at $E_{pa2} = +1.159$ V is observed for **1** due to irreversible oxidation of $Cu^{II} \rightarrow Cu^{III}$.[47] The cyclic voltammogram of complex **2** (Figure 3) exhibits an electrochemically irreversible $Co^{III} \rightarrow Co^{II}$ reduction at $E_{pc} = -0.71$ V. Upon reversal of the scan direction, the Co(II) complex is reoxidized to Co(III) at $E_{pa} = +0.11$ V. The peak separation between the related cathodic and anodic waves

Table 2. IR Spectral Data (cm^{-1}) of Ligand H_2L^1 and of Complexes **1** and **2**

Compound	ν(C=N)	ν(C–$O_{Phenolic}$)	ν(O–H/H_2O)	ν(M–N)	ν(N–H)	ν(ClO_4^-)
H_2L^1	1635	1260	3449	—	—	—
1	1610	1226	3432	438	—	—
2	1591	1234	—	459	3232–3148	1081

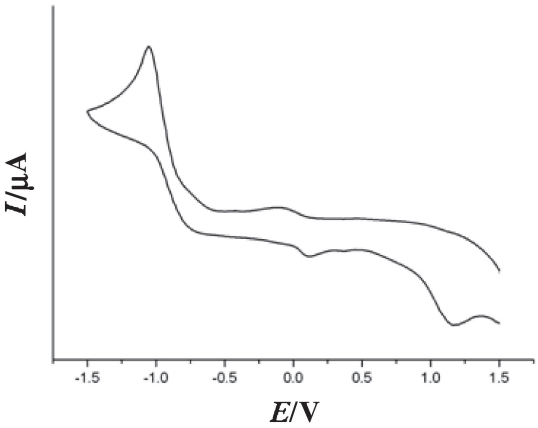

Figure 2. Cyclic voltammogram of **1** at a scan rate of 100 mV s^{-1}.

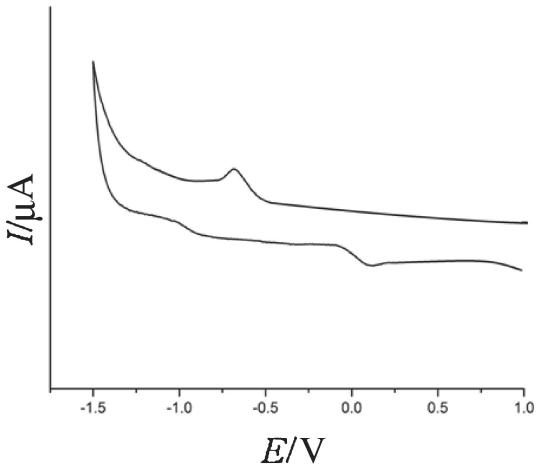

Figure 3. Cyclic voltammogram of **2** at a scan rate of 100 mV s^{-1}.

indicates clearly the irreversible nature of the redox reaction Co^{III}/Co^{II} ($\Delta E_p = 820$ mV).[48]

Crystal Structure of $[Cu(L^1)]\cdot H_2O$ (1) and $[Co(L^1)(HL^2)]ClO_4\cdot CH_3CN$ (2). The crystal structure of **1** is shown in Figure S1 and selected bond distances and angles are listed in Table S2. In complex **1**, the Schiff base adopts an almost planar geometry with the Cu(II) ion located at the inner N_2O_2 cavity of the bicompartmental ligand. The square-planar copper(II) center is coordinated by phenoxo oxygens and by imino nitrogen atoms of the doubly deprotonated ligand $[L^1]^{2-}$. Due to conformational freedom of the propylenediamine unit, the two halves of the salen-type ligand are tilted forming a dihedral angle of 37.7°. An interesting structural feature of solid state is the bifurcated H-bonds assisted by the lattice water molecule as shown in Figure S1, where the $O_{(H_2O)}\cdots O$ distances are in between 2.84–3.22 Å (Table S3).

Structural aspects of **1** closely resembles that of Cu(II) complex published by Cristóvão et al.[39] The average Cu–N (1.967 Å) and Cu–O (1.914 Å) bond distances in **1** are similar to the reported values (Cu–N 1.963 Å and Cu–O 1.914 Å). Likewise, bond angles [86.60(12)–158.03(12)°] are close comparable to those in the reported Cu(II) complex [86.7(1)–158.2(1)°]. However single crystals of **1** were obtained from the reaction mixture in methanol, while Cristóvão et al. recrystallized it from dimethylformamide.

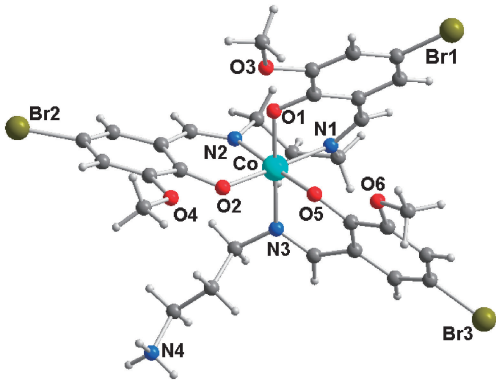

Figure 4. Perspective view of the cationic complex of **2** (C atoms not labeled and the lattice acetonitrile molecule not shown for sake of clarity).

Table 3. Selected Bond Distances (Å) and Bond Angles (degree) in $[Co(L^1)(HL^2)]ClO_4\cdot CH_3CN$ (**2**)

Bond distances/Å			
Co–N1	1.920(8)	Co–O1	1.894(5)
Co–N2	1.925(8)	Co–O2	1.916(7)
Co–N3	1.948(7)	Co–O5	1.901(6)
Bond angles/degree			
N1–Co–N2	91.0(4)	N2–Co–O5	176.9(3)
N1–Co–N3	92.9(3)	N3–Co–O1	175.1(3)
N1–Co–O1	90.0(3)	N3–Co–O2	91.6(3)
N1–Co–O2	173.4(3)	N3–Co–O5	88.8(3)
N1–Co–O5	90.0(3)	O1–Co–O2	85.2(2)
N2–Co–N3	94.1(3)	O1–Co–O5	87.2(3)
N2–Co–O1	89.8(3)	O2–Co–O5	85.3(3)
N2–Co–O2	93.5(4)		

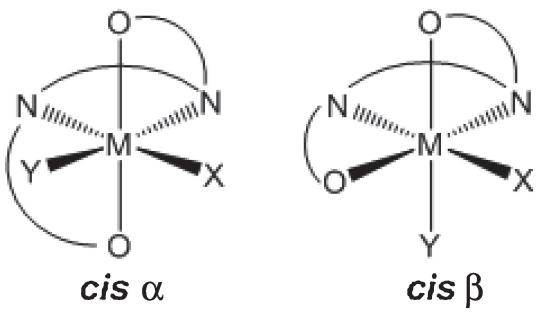

Scheme 1. *cis* Conformation of the ligands in metal complex.

The structure of $[Co(L^1)(HL^2)]ClO_4\cdot CH_3CN$ (**2**) consists of a discrete $[Co(L^1)(HL^2)]^+$ monocation together with a perchlorate anion and a lattice molecule of acetonitrile. It can be considered as a unique complex where the mono-condensed Schiff base ligand HL^2 (Figure 1) is simultaneously present with the di-condensed ligand, H_2L^1. The molecular structure of the cationic complex is shown in Figure 4 and relevant bond length and angle data are listed in Table 3. With respect to the structure of complex **1**, here the salen-type ligand L^1 assumes a β-*cis* folded configuration (Scheme 1).[49–51] This arrangement

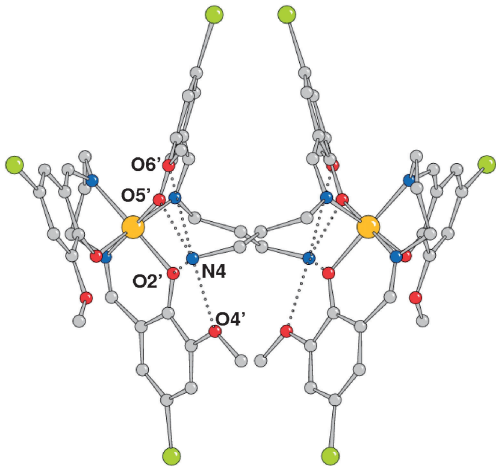

Figure 5. Crystal packing of **2** showing the cooperative H-bonds between the NH_3^+ groups with oxygen atoms of the symmetry related complex. Primed atoms at $1/2 - x$, y, $1 - z$.

is likely favored to allow the bidentate chelating ligand HL^2 to occupy two *cis* sites in the coordination sphere, similarly as observed for the (acetylacetonato)(salen)cobalt(III).[51] It was suggested that such configuration leads to a significantly reduced electron density delocalization in the two moieties of $Co(L^1)$.[49] The HL^2 ligand is present in its zwitterionic form, having the amino group protonated (Figure 1). This mixed-ligand Schiff base complex is chiral, although the product is a racemic mixture. The overall geometry of the N_3O_3 chromophore is a distorted octahedron where each oxygen is *trans* located to a N donor. The equatorial plane is outlined by the two phenoxo oxygens (O1, O5) and the imine nitrogens (N2, N3), whereas another phenoxo oxygen (O2) and imine nitrogen (N1) occupy the axial sites of the octahedron. The corresponding bond angle O2–Co–N1 of 173.4(3)° shows the larger deviation from the ideal value of 180°. The Co–N and Co–O distances are comparable with those of similar complexes.[50–53] However despite the apparent almost regular octahedron, the di-condensed ligand (L^1) manifest some distortions (likely induced by packing requirements) and the two half moieties form a dihedral angle of 56.25(9)°, far from the ideal value of 90°.

The crystal packing shows that the units are arranged in pair about a crystallographic twofold axis connected by intermolecular N–H···O hydrogen bonds as shown in Figure 5. The amine group interacts with the phenoxo O2, O5 and with the methoxo oxygen atoms O4 and O6, and in addition with perchlorate anions (not shown in Figure 4). The H-bond geometric parameters are listed in Table 4.

In both complexes **1** and **2** it is interesting to observe that all methoxy groups are coplanar with the phenyl ring suggesting the presence of a conjugation effect.[54]

We have synthesized a bis-Schiff base ligand, H_2L^1 by the 1:2 condensation of 1,3-diaminopropane and 5-bromo-*o*-vanillin in methanol and allowed its separate reactions with copper(II) and cobalt(II) salts. The compositions and structures of the resulting two complexes are considerably different for the two metal ions. In the first case, a simple mononuclear

Table 4. Hydrogen Bond Dimensions for Complex $[Co(L^1)(HL^2)]ClO_4 \cdot CH_3CN$ (**2**)[a)]

D–H···A	*d*(D–H) /Å	*d*(H···A) /Å	*d*(D···A) /Å	∠(DHA) /°
N4–H4B···O2	0.890	2.34	3.001(9)	131
N4–H4B···O4	0.890	2.02	2.821(10)	150
N4–H4C···O5	0.890	1.92	2.710(9)	146
N4–H4C···O6	0.890	2.33	3.022(10)	135
N4–H4A···O11	0.890	2.25	3.039(13)	148
N4–H4A···O13	0.890	2.47	3.169(12)	136

a) Symmetry code for A in all cases: $1/2 - x$, y, $1 - z$.

square-planar Cu(II) complex is produced, while in the second we obtained a novel mixed-ligand cationic complex $[Co(L^1)(HL^2)]^+$ where both di- and mono-condensed Schiff base ligands, $(L^1)^{2-}$ and HL^2, coexist in the same monomeric Co(III) system. The more evident difference between complexes **1** and **2** is represented (beside the different coordination geometry) by the tetradentate H_2L^1 ligand that assumes an almost planar geometry in **1** and a folded *cis*-β configuration (Scheme 1) in **2**. The latter is induced by the presence of the ancillary chelating ligand HL^2.

From the above results it is evident that the di-condensed Schiff base ligand is stable enough to form the copper(II) complex, while it is partially converted to the corresponding mono-condensed ligand to yield the cobalt(III) complex. It has been found that in some cases tetradentate Schiff base ligands undergo hydrolytic cleavage leading to mono-condensed ligand.[55] But the coexistence of mono- and bis-Schiff bases in the same complex as reported here for **2**, is still infrequent in the literature.[48] Complex **2** has been prepared through a direct reaction involving $Co(ClO_4)_2 \cdot 6H_2O$ and the corresponding ligand with 1:2 molar ratio in methanol/acetonitrile medium under aerobic conditions. The starting cobalt(II) salt apparently undergoes aerial oxidation in presence of the π-acceptor Schiff base to generate a Co^{III} derivative. As already known, low-spin cobalt(III) prefers six-coordinate octahedral geometry as indicated by the crystal field stabilization energy (CFSE). Here, it is not possible for the tetradentate ligand H_2L^1 to satisfy solely all the six coordination sites of Co(III) in presence of noncoordinating perchlorate ion. Consequently, cobalt(III) ion induces the in situ generation of tridentate mono-condensed ligand HL^2 through the hydrolytic cleavage of one of the imine bonds of di-condensed Schiff base H_2L^1, and in principle both the ligands can generate a discrete octahedral complex avoiding steric crowding. On the contrary, copper(II), being a d^9 system, is liable to experience an active Jahn–Teller effect that makes its coordination number and geometry much more flexible and therefore, it can form a variety of complexes with either tri- or tetradentate Schiff base ligand.

Catalytic Epoxidation of Alkenes. The ability of complexes **1** and **2** to catalyze the oxidation of alkenes was investigated using H_2O_2 and PhIO as oxidants. To select the appropriate solvent for the reaction, the oxidation of styrene with PhIO was carried out in various solvents. Among CH_3CN, CH_3OH, and DMF, the former was chosen as the reaction medium, because of the higher oxidation yield observed (Table 5). The two complexes were shown to be efficient catalysts for

Table 5. Effect of Solvent on the Oxidation of Styrene with PhIO Catalyzed by **1** and **2**[a)]

Solvent	Catalyst	Conversion[b)]/%
CH_3CN	**1**	75
	2	79
DMF	**1**	65
	2	68
CH_3OH	**1**	34
	2	36

a) Reaction conditions: alkene (0.5 mmol); catalyst (2 μmol); PhIO (1.0 mmol); $T = 20$ °C; solvent (4 mL); $t = 2$ h. b) Disappearance of starting material after 2 h.

Table 6. Oxidation of Alkenes with PhIO Catalyzed by **1** and **2**[a),b)]

Alkene	Catalyst	Conversion[c)] /%	t.o.n.[d)]	k_{cat} /min^{-1}
cis-Stilbene	**1**	71	178	0.0117(8)
	2	73	182	0.0121(7)
Styrene	**1**	75	188	0.0133(7)
	2	79	198	0.0143(6)
Cyclohexene	**1**	91	228	0.0203(9)
	2	95	238	0.0245(7)
trans-4-Octene	**1**	100	250	0.033(1)
	2	100	250	0.041(1)

a) Reaction conditions: alkene (0.5 mmol); catalyst (2 μmol); PhIO (1.0 mmol); $T = 20$ °C; $t = 2$ h; solvent: CH_3CN. b) Oxidation product: epoxide. c) Disappearance of starting material after 2 h. d) t.o.n.: amount of epoxide/amount of catalyst.

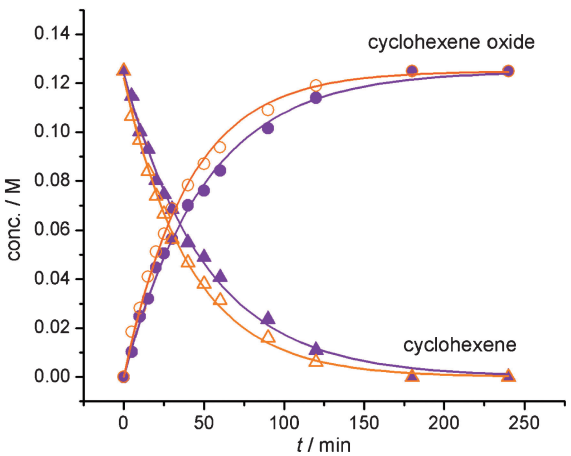

Figure 6. Reaction profiles of the cyclohexene oxidation with PhIO catalyzed by **1** (solid symbols) and **2** (open symbols) in CH_3CN, at 20 °C. Solid lines correspond to first-order fit of experimental data. Experimental conditions: 0.5 mmol of cyclohexene, 1 mmol of PhIO, 0.4 mol of catalyst, and 4 mL of CH_3CN.

alkene oxidation with PhIO as oxidant. Under conditions summarized in Table 6, the four tested alkenes were selectively oxidized to the corresponding epoxides with turnovers in the range of 178–250, after 2 h of reaction. In spite of structural differences, the two catalysts showed the same epoxide selectivity and similar alkene epoxidation rates. In each case,

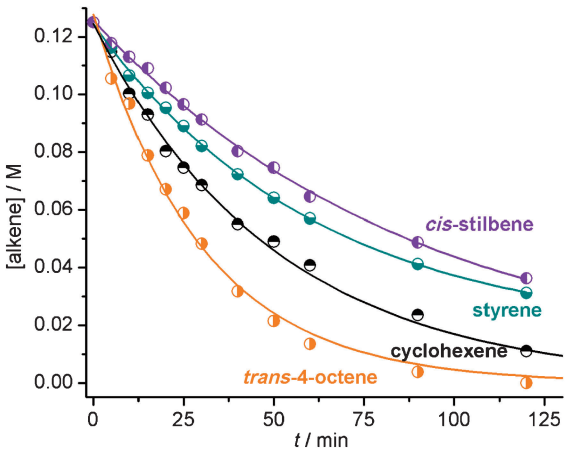

Figure 7. Kinetic profiles for the alkene oxidation with PhIO catalyzed by **1** in CH_3CN, at 20 °C. Solid lines correspond to first-order fit of experimental data. Experimental conditions: 0.5 mmol of alkene, 1 mmol of PhIO, 0.4 mol % catalyst, and 4 mL of CH_3CN.

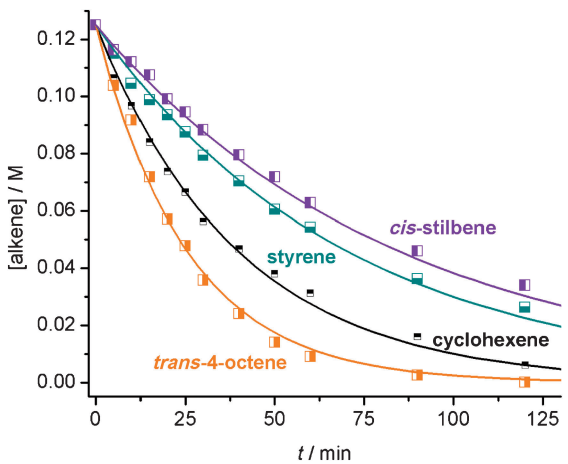

Figure 8. Kinetic profiles for the alkene oxidation with PhIO catalyzed by **2** in CH_3CN, at 20 °C. Solid lines correspond to first-order fit of experimental data. Experimental conditions: 0.5 mmol of alkene, 1 mmol of PhIO, 0.4 mol % catalyst, and 4 mL of CH_3CN.

2 proved to be a slightly better catalyst than **1**, as shown for cyclohexene oxidation in Figure 6. For the two complexes, the relative oxidation rates follow the trend *trans*-4-octene > cyclohexene > styrene > *cis*-stilbene, and the pseudo-first-order rate constants calculated from kinetic curves (Figures 7 and 8) are listed in the last column of Table 6. The observed trend indicates that the catalysts favor the oxidation of more electron-rich substrates over less, and suggests an electrophilic character for the active site of catalysts. The catalytic constants determined for **1** and **2** are several order higher than those found for the PhIO oxidation of alkenes catalyzed by Cu–salen complexes in Cl_2CH_2 at 30 °C,[32] and by Co–salen compounds in Cl_2CH_2 at 25 °C.[56] Other Co and Cu complexes evaluated as catalysts for PhIO oxidation of alkenes are listed in Table S4.[32,35,56–59] A common feature of these complexes is their planar geometry around the metal center imposed by the ligand. An inspection of Tables 6 and S4 shows that alkene

conversions and epoxide yields achieved with **1** and **2** are better than for Co and Cu complexes listed in Table S4. It has been observed that the *cis*-β and *cis*-α folded conformation of a tetradentate Schiff base ligand stabilizes higher oxidation states of the metal center better than the ligand arranged in the equatorial plane of a tetragonal complex.[60,61] In the case of complex **2**, the effect of the ligand arrangement around the metal center shifts the Co(III) to Co(II) toward the negative potentials side relative to square-planar Co complexes, resulting in a stabilizing effect of the higher oxidation state. This fact correlates with the enhanced activity observed for this complex compared to the Co–salen counterpart. Therefore, the *cis*-β conformation of the Schiff base ligand facilitates the formation of oxidized Co(V) species yielding a more efficient catalyst for alkene epoxidation than Co(III)-complexes with the ligand disposed in the equatorial plane. The increased flexibility of the ligand environment in **1** compared to Cu–salen, also stabilizes higher oxidation states of the copper center[62] and can correlate with the fact that **1** is a more efficient catalyst than complexes reported in Table S4, where the metal is in the planar geometry imposed by the ligand.

It has been found that electron-withdrawing substituents *para* to the phenolato improve catalytic activity and rise alkene oxidation rates,[32,59] while the nature of the substituent at the *ortho* position does not affect the oxidation rate, the catalytic activity being affected only in the case of the bulkiest *o*-^{t}Bu group.[59] Therefore, for complexes **1** and **2**, the 5-Br substituent in the ligand increases the ability of the metal center to activate the terminal oxidant.

Co(III) complexes are better catalysts for PhIO oxidation of alkenes than Cu(II) complexes with the same ligand.[32,58] A suitable explanation for the similar activity of **1** and **2** is that in the case of $[Co(L^1)(HL^2)]^+$ the formation of the metal–oxidant adduct requires ligand substitution, while CuL^1 possesses vacant positions. Thus, whereas Co(III) in **2** is better to activate the oxidant, binding of the terminal oxidant to the metal center is favored in **1**. The compensation of these two factors results in two catalysts of approximately similar activity, with the Co(III) complex being slightly better than the Cu(II) one.

Catalysts **1** and **2** proved to be active after complete conversion of the alkene (2 h for *trans*-4-octene, 3 h for cyclohexene, 4 h for styrene and *cis*-stilbene), since a new addition of alkene resulted in conversion to epoxide with retention of efficiency. The fact that the catalysts retain their activity after the second addition evidences their robustness, affording twice the turnover number (t.o.n.) (converted mol of alkene/mol metal catalyst) of the first run. This result is in line with the analogous electronic spectra taken before and at the end of the reaction, indicating that the starting complexes are the true catalysts. When H_2O_2 was used as the oxygen source, CH_3CN was also the solvent of choice. With this oxidant, alkenes are selectively converted into the epoxide in the presence of **1** or **2**. However, oxidation is slow and complete conversion takes one (aliphatic alkenes) or two days (aromatic alkenes) (Table 7). The low rates of H_2O_2-epoxidation of alkenes catalyzed by these complexes can be attributed to catalyst deactivation in aqueous medium and partial H_2O_2 disproportionation. Here again, activation of peroxide is better in the Co(III) complex, while binding of peroxide to the metal center is facilitated in the Cu(II) complex, resulting in two catalysts of similar activity, with **2** being slightly better than **1**.

Table 7. Oxidation of Alkenes with H_2O_2 Catalyzed by **1** and **2**[a),b)]

Alkene	Catalyst	Time /h	Conversion[c)] /%	t.o.n.[d)]
cis-Stilbene	**1**	6	5	20
		12	20	80
		24	51	204
		48	100	400
	2	6	7	28
		12	26	104
		24	57	228
		48	100	400
Styrene	**1**	6	7	28
		12	24	96
		24	55	220
		48	100	400
	2	6	10	40
		12	31	124
		24	59	236
		48	100	400
Cyclohexene	**1**	6	25	100
		12	48	192
		24	100	400
	2	6	30	120
		12	57	228
		24	100	400
trans-4-Octene	**1**	6	15	60
		12	39	156
		24	100	400
	2	6	25	100
		12	46	184
		24	100	400

a) Reaction conditions: alkene (0.8 mmol); catalyst (2 mmol); H_2O_2 (1.5 mmol); $T = 0$ °C; solvent: CH_3CN. b) Oxidation product: epoxide. c) Disappearance of starting material. d) t.o.n.: amount of epoxide/amount of catalyst.

Results obtained for the PhIO and H_2O_2 oxidation of alkenes catalyzed by $[Co(L^1)(HL^2)]^+$ make clear that the lack of vacant or labile sites on Co(III) is not a limitation to show activity, a fact already documented for the aerobic oxidation of alkenes catalyzed by a six-coordinated Co(III) complex.[63] Both the Cu(II) and Co(III) catalysts activate the oxidant (H_2O_2 or PhIO) for transferring an oxygen atom to the alkene. The activation may initiate through binding of peroxide or PhIO to the metal complex to form an adduct upon substitution of a labile solvent molecule (in complex **1**) or by ligand shift (in complex **2**). This oxidant–metal complex adduct may serve as the reactive species responsible for the oxygen atom transfer to the alkene[64] or to be the precursor of a high-valent metal-oxo species in the oxygenation reaction.[56]

Conclusion

In conclusion this paper describes the different coordination behavior of a di-condensed Schiff base ligand H_2L^1 upon reaction with two different metal ions, copper(II) and cobalt(III). It was observed that the tetradentate ligand remains

intact giving rise to the square-planer copper(II) complex **1**. But upon reaction with cobalt salt, the ligand undergoes partial hydrolysis to the mono-condensed ligand HL^2 furnishing an octahedral cobalt(III) complex **2**. The formation of such an exclusive mixed–ligand complex can be explained by the tendency of cobalt(III) template to achieve octahedral coordination. Both the complexes, despite of their structural diversities, are found to be active catalysts in the epoxidation of *cis*-stilbene, styrene, cyclohexene, and *trans*-4-octene by using PhIO as oxidant.

M. Maiti is thankful to the UGC, Government of India, for providing her with the financial support to carry out the work.

Supporting Information

The Supporting Information contains Table S1, S2, S3, S4 and Figure S1 about crystal information of **1** and **2**. This material is available electronically on J-STAGE.

References

1 R. D. Jones, D. A. Summerville, F. Basolo, *Chem. Rev.* **1979**, *79*, 139.
2 G. Henrici-Olivé, S. Olivé, *The Chemistry of the Catalyzed Hydrogenation of Carbon Monoxide*, Springer, Berlin, **1984**. doi:10.1007/978-3-642-69662-6.
3 H. Dugas, C. Penney, *Bioorganic Chemistry: A Chemical Approach to Enzyme Action*, Springer, New York, **1981**. doi:10.1007/978-1-4684-0095-3.
4 J. D. Margerum, L. J. Miller, *Photochromism*, Wiley Interscience, New York, **1971**.
5 J.-P. Costes, F. Dahan, A. Dupuis, J.-P. Laurent, *Inorg. Chem.* **1997**, *36*, 4284.
6 J.-P. Costes, F. Dahan, A. Dupuis, J.-P. Laurent, *Chem.—Eur. J.* **1998**, *4*, 1616.
7 G. Novitchi, S. Shova, A. Caneschi, J.-P. Costes, M. Gdaniec, N. Stanica, *Dalton Trans.* **2004**, 1194.
8 R. Koner, H.-H. Lin, H.-H. Wei, S. Mohanta, *Inorg. Chem.* **2005**, *44*, 3524.
9 H.-D. Bian, J.-Y. Xu, W. Gu, S.-P. Yan, P. Cheng, D.-Z. Liao, Z.-H. Jiang, *Polyhedron* **2003**, *22*, 2927.
10 M. S. Ray, G. Mukhopadhyay, M. G. B. Drew, T.-H. Lu, S. Chaudhuri, A. Ghosh, *Inorg. Chem. Commun.* **2003**, *6*, 961.
11 P. Mukherjee, M. G. B. Drew, A. Ghosh, *Eur. J. Inorg. Chem.* **2008**, 3372.
12 S. Sen, P. Talukder, S. K. Dey, S. Mitra, G. Rosair, D. L. Hughes, G. P. A. Yap, G. Pilet, V. Gramlich, T. Matsushita, *Dalton Trans.* **2006**, 1758.
13 S. Leininger, B. Olenyuk, P. J. Stang, *Chem. Rev.* **2000**, *100*, 853.
14 W. Meier, *Chem. Soc. Rev.* **2000**, *29*, 295.
15 T. Steiner, *Angew. Chem., Int. Ed.* **2002**, *41*, 48.
16 G. R. Desiraju, *Acc. Chem. Res.* **2002**, *35*, 565.
17 C. Janiak, *J. Chem. Soc., Dalton Trans.* **2000**, 3885.
18 Z. D. Tomić, D. Sredojević, S. D. Zarić, *Cryst. Growth Des.* **2006**, *6*, 29.
19 D. N. Sredojević, Z. D. Tomić, S. D. Zarić, *Cryst. Growth Des.* **2010**, *10*, 3901.
20 *Aziridines and Epoxides in Organic Synthesis*, ed. by A. K. Yudin, Wiley-VCH, Weinheim, Germany, **2006**. doi:10.1002/3527607862.
21 K. Weissermel, H.-J. Arpe, *Industrial Organic Chemistry*, Wiley-VCH, Weinheim, Germany, **1997**.
22 R. A. Sheldon, H. van Bekkum, *Fine Chemicals through Heterogeneous Catalysis*, Wiley-VCH, Weinheim, Germany, **2001**. doi:10.1002/9783527612963.index.
23 W. Al-Maksoud, S. Daniele, A. B. Sorokin, *Green Chem.* **2008**, *10*, 447.
24 E. N. Jacobsen, A. Pfaltz, H. Yamamoto, *Comprehensive Asymmetric Catalysis*, Springer, Berlin, Germany, **1999**.
25 H. Nishikori, C. Ohta, T. Katsuki, *Synlett* **2000**, 1557.
26 M. J. Sabater, A. Corma, A. Domenech, V. Fornés, H. García, *Chem. Commun.* **1997**, 1285.
27 D. Sadhukhan, A. Ray, G. Pilet, C. Rizzoli, G. M. Rosair, C. J. Gómez-García, S. Signorella, S. Bellú, S. Mitra, *Inorg. Chem.* **2011**, *50*, 8326, and references therein.
28 P. Karandikar, M. Agashe, K. Vijayamohanan, A. J. Chandwadkar, *Appl. Catal., A* **2004**, *257*, 133.
29 S. Koner, *Chem. Commun.* **1998**, 593.
30 S. Jana, B. Dutta, R. Bera, S. Koner, *Langmuir* **2007**, *23*, 2492.
31 G. Das, R. Shukla, S. Mandal, R. Singh, P. K. Bharadwaj, J. van Hall, K. H. Whitmire, *Inorg. Chem.* **1997**, *36*, 323.
32 S. Zolezzi, E. Spodine, A. Decinti, *Polyhedron* **2003**, *22*, 1653.
33 C. Adhikary, R. Bera, B. Dutta, S. Jana, G. Bocelli, A. Cantoni, S. Chaudhuri, S. Koner, *Polyhedron* **2008**, *27*, 1556.
34 S. Bunce, R. J. Cross, L. J. Farrugia, S. Kunchandy, L. L. Meason, K. W. Muir, M. O'Donnell, R. D. Peacock, D. Stirling, S. J. Teat, *Polyhedron* **1998**, *17*, 4179.
35 X.-H. Lu, Q.-H. Xia, H.-J. Zhan, H.-X. Yuan, C.-P. Ye, K.-X. Su, G. Xu, *J. Mol. Catal. A: Chem.* **2006**, *250*, 62.
36 S. Rayati, S. Zakavi, M. Koliaei, A. Wojtczak, A. Kozakiewicz, *Inorg. Chem. Commun.* **2010**, *13*, 203.
37 B. K. Das, R. Chakrabarty, *J. Chem. Sci.* **2011**, *123*, 163.
38 N. Gimeno, R. Vilar, *Coord. Chem. Rev.* **2006**, *250*, 3161.
39 B. Cristóvão, B. Miroslaw, J. Kłak, *Polyhedron* **2013**, *62*, 218.
40 M. Maneiro, M. R. Bermejo, A. Sousa, M. Fondo, A. M. González, A. Sousa-Pedrares, C. A. McAuliffe, *Polyhedron* **2000**, *19*, 47.
41 CrysAlis-RED 170, Oxford-Diffraction, **2002**.
42 Z. Otwinowski, W. Minor, in *Macromolecular Crystallography Part A* in *Methods in Enzymology*, ed. by C. W. Carter, Jr., R. M. Sweet, Academic Press, New York, **1997**, Vol. 276, pp. 307–326. doi:10.1016/S0076-6879(97)76066-X.
43 A. Altomare, M. C. Burla, M. Camalli, G. L. Cascarano, C. Giacovazzo, A. Guagliardi, A. G. G. Moliterni, G. Polidori, R. Spagna, *J. Appl. Crystallogr.* **1999**, *32*, 115.
44 G. M. Sheldrick, *SHELX-97*, University of Göttingen, Göttingen, Germany, **1997**.
45 D. J. Watkin, C. K. Prout, J. R. Carruthers, P. W. Betteridge, *CRYSTALS*, Chemical Crystallography Laboratory, Oxford, U.K., **1999**, Issue 11.
46 A. B. P. Lever, *Inorganic Electronic Spectroscopy*, 2nd ed., Elsevier, Amsterdam, **1984**.
47 M. Maiti, D. Sadhukhan, S. Thakurta, S. Sen, E. Zangrando, R. J. Butcher, R. C. Deka, S. Mitra, *Eur. J. Inorg. Chem.* **2013**, 527.
48 S. Thakurta, R. J. Butcher, G. Pilet, S. Mitra, *J. Mol. Struct.* **2009**, *929*, 112.
49 T. Katsuki, *Chem. Soc. Rev.* **2004**, *33*, 437.
50 R. Dreos, P. Siega, *Organometallics* **2006**, *25*, 5180.

51 M. Calligaris, G. Manzini, G. Nardin, L. Randaccio, *J. Chem. Soc., Dalton Trans.* **1972**, 543.
52 J. P. Corden, W. Errington, P. Moore, M. G. H. Wallbridge, *Chem. Commun.* **1999**, 323.
53 R. Dreos, G. Nardin, L. Randaccio, P. Siega, G. Tauzher, V. Vrdoljak, *Inorg. Chem.* **2003**, *42*, 6805.
54 W. Hummel, K. Huml, H.-B. Bürgi, *Helv. Chim. Acta* **1988**, *71*, 1291.
55 S. Gourbatsis, S. P. Perlepes, I. S. Butler, N. Hadjiliadis, *Polyhedron* **1999**, *18*, 2369.
56 J. D. Koola, J. K. Kochi, *J. Org. Chem.* **1987**, *52*, 4545.
57 J. Adhikary, A. Guha, T. Chattopadhyay, D. Das, *Inorg. Chim. Acta* **2013**, *406*, 1.
58 L. F. Lima, M. L. Corraza, L. Cardozo-Filho, H. Márquez-Alvarez, O. A. C. Antunes, *Braz. J. Chem. Eng.* **2006**, *23*, 83.
59 C.-W. Ho, W.-C. Cheng, M.-C. Cheng, S.-M. Peng, K.-F. Cheng, C.-M. Che, *J. Chem. Soc., Dalton Trans.* **1996**, 405.
60 V. Daier, D. Moreno, C. Duhayon, J.-P. Tuchagues, S. Signorella, *Eur. J. Inorg. Chem.* **2010**, 965.
61 K. J. Schenk, S. Meghdadi, M. Amirnasr, M. H. Habibi, A. Amiri, M. Salehi, A. Kashi, *Polyhedron* **2007**, *26*, 5448.
62 M. K. Taylor, J. Reglinski, L. E. A. Berlouis, A. R. Kennedy, *Inorg. Chim. Acta* **2006**, *359*, 2455.
63 D. Saha, T. Maity, R. Bera, S. Koner, *Polyhedron* **2013**, *56*, 230.
64 C. Wang, T. Kurahashi, H. Fujii, *Angew. Chem., Int. Ed.* **2012**, *51*, 7809.